

Electronic Supplementary Information

## Dual function interfacial layer for highly efficient and stable lead halide perovskite solar cells

Dandan Song,<sup>a</sup> Dong Wei,<sup>a</sup> Peng Cui,<sup>a</sup> Meicheng Li,<sup>a,b\*</sup> Zhiqiang Duan,<sup>a</sup> Tianyue Wang,<sup>a</sup> Jun Ji,<sup>a</sup> Yaoyao Li,<sup>a</sup> Joseph Michel Mbengue,<sup>a</sup> Yingfeng Li,<sup>a</sup> Yue He<sup>a</sup>, Mwenya Trevor<sup>a</sup> and Nam-Gyu Park<sup>c</sup>

<sup>a</sup> State Key Laboratory of Alternate Electrical Power System with Renewable Energy Sources, School of Renewable Energy, North China Electric Power University, Beijing 102206, China.

<sup>b</sup> Chongqing Materials Research Institute, Chongqing 400707, China

<sup>c</sup> School of Chemical Engineering and Department of Energy Science, Sungkyunkwan University (SKKU), Suwon, 440-746, Korea.

\* Corresponding author: E-mail: mcli@ncepu.edu.cn; Fax: +86 10 6177 2951; Tel: +86 10 6177 2951.

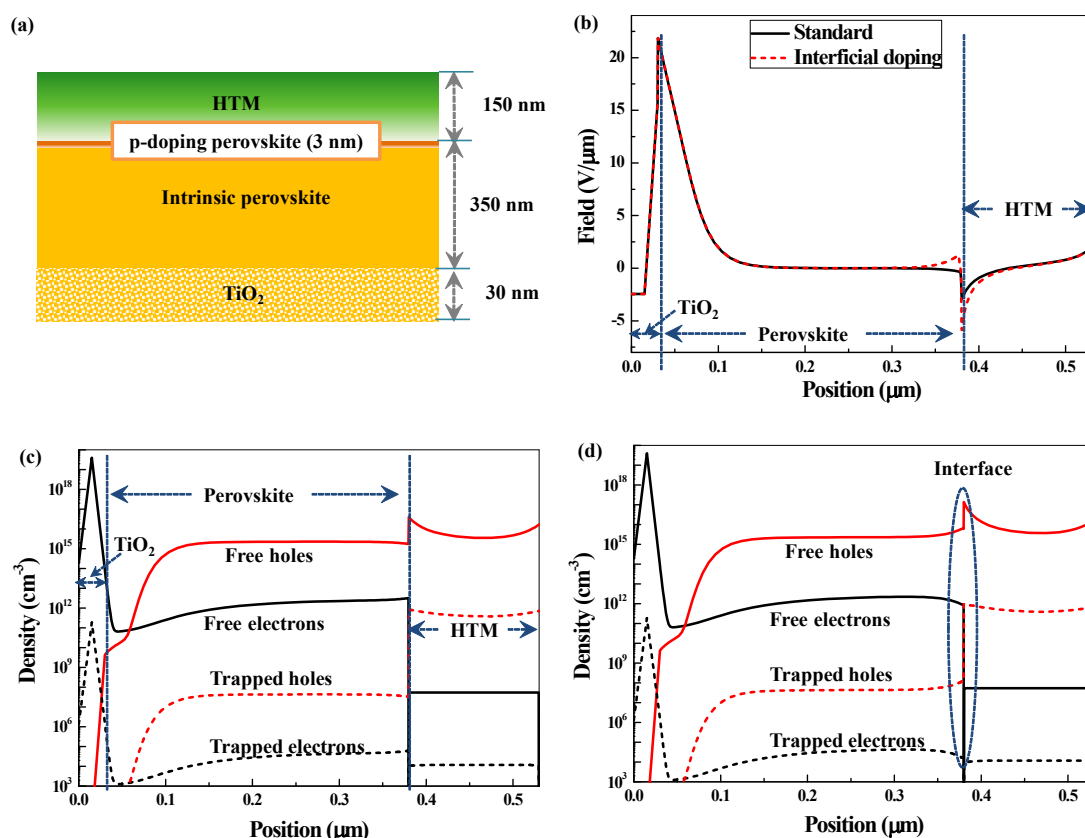


Fig. S1 Simulated electric field and carrier distribution in the perovskite solar cells (PSCs) without or with an interface p-type doped perovskite (3nm) by wxAMPS. (a) The schematic device structure used for simulation. (b) Electric field distribution. (c, d) Carrier distribution without (c) or with interfacial doping layer (d). It is shown that the density of the free electrons and the trapped electrons can be reduced by the p-type doped perovskite at the perovskite/HTM interface, demonstrating the role of the p-type doped perovskite in blocking electrons and suppressing the electron trapping.

To study the cause of high performance of the modified PSCs, the electrical parameters including series resistance ( $R_s$ ), shunt resistance ( $R_{sh}$ ) and inverse saturation current ( $J_0$ ) of the PSCs extracted from photo J-V curves (Table S1) were investigated. From Table S1 it appears that all of the electrical parameters are improved in the modified devices. Low series resistance ( $R_s$ ) in modified device reflects low bulk resistance, which favors high  $J_{SC}$  and FF. High shunt resistance ( $R_{sh}$ ) reflects less defects in the modified device, which facilitates high  $V_{OC}$  and FF. Therefore, high PCE is obtained in the modified devices. The reverse saturation current ( $J_0$ ) correlates with the carrier recombination in p- region and n-region, so lower  $J_0$  in modified device corresponds to lower carrier recombination in these regions. Considering the fact that F4TCNQ can only modify

the perovskite close to perovskite/HTM interface, the improved electrical parameters derive from the reduced carrier recombination distributing attached to the interface.

Table S1 Fitted electrical parameters of the PSCs without (standard) or with F4TCNQ modification (modified)<sup>a</sup>.

PSCs	$R_s$ ( $\Omega \text{ cm}^2$ )	$R_{sh}$ ( $\text{k}\Omega \text{ cm}^2$ )	$J_0$ ( $\text{mA cm}^{-2}$ )	$J_{sc}$ ( $\text{mA cm}^{-2}$ )	$m$
Standard	4.46	0.90	$1 \times 10^{-5}$	19.9	2.76
Modified	1.15	2.75	$3 \times 10^{-6}$	20.9	2.64

<sup>a</sup> The parameters were obtained by fitting the experimental photocurrent-voltage curves of the PSCs

(Fig. 4b) to the equation  $J = J_{sc} - J_0 \left( \exp \frac{-q(V + AJR_s)}{mk_B T} - 1 \right) - \frac{V + AJR_s}{AR_{sh}}$ , where  $A$  and  $m$  represent for device area and diode ideality factor, respectively.

The calculated ideality factor of the PSCs is larger than 2 (Table S1), in which case the recombination current in the space charge region makes main contribution to the dark current. In addition, the recombination in the space charge region of the PSCs is governed by trap states<sup>1</sup>. From Fig. S2a, the dark current in the space charge limited region of standard solar cell within low voltage range is higher than of modified solar cell, indicating more severe recombination and trap states contained in the space charge region of the former. Hence, it is able to be inferred that the density of the traps states are reduced in the modified perovskite, which confirming the function of F4TCNQ in enhancing the built-in potential and reducing the trap states in the PSCs

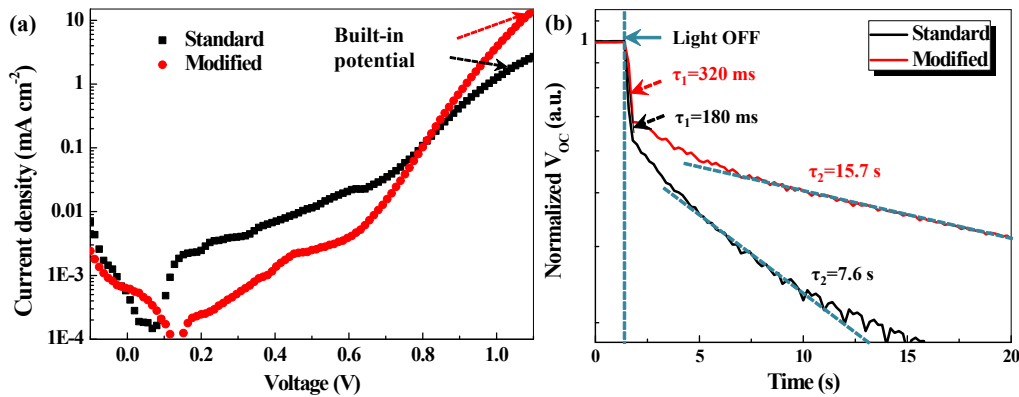


Fig. S2 (a) Dark J-V curves of the standard and modified PSCs. (b) OCVD curves of the standard and modified PSCs. The decay of  $V_{oc}$  after the incident light off is governed by two processes with different time domains. The fast decay ( $\tau_1$ ) in ms time scale can be associated with the trap-induced recombination, which consumes the photogenerated carriers immediately with light off, leading to the

decreased  $V_{OC}$ . The slow decay ( $\tau_2$ ) in the long time scale is probably associated with the ferroic behaviour of the perovskite<sup>2</sup>.

Furthermore, open-circuit voltage decay (OCVD) characters also reveal the reduced carrier recombination in modified PSCs. As shown in Fig. S2b, the fitted decay lifetime of  $V_{OC}$  is obviously higher in modified PSC (320 ms) than in standard one (180 ms), implying slow recombination of the photogenerated carriers in the former. Moreover, the built-in potential estimated from dark J-V curves<sup>3</sup> (Fig. S2a) is higher in modified PSCs (1.1 V) than that in standard PSCs (1.0 V), indicating the function of F4TCNQ in interfacial doping of perovskite at perovskite/HTM interface. Hence, the suppressed carrier recombination and the interfacial doping lead to high  $V_{OC}$  of the modified PSCs, while the reduction of the trap states decreases carrier loss and increases  $J_{SC}$ , leading to the resultant increase in FF and PCE.

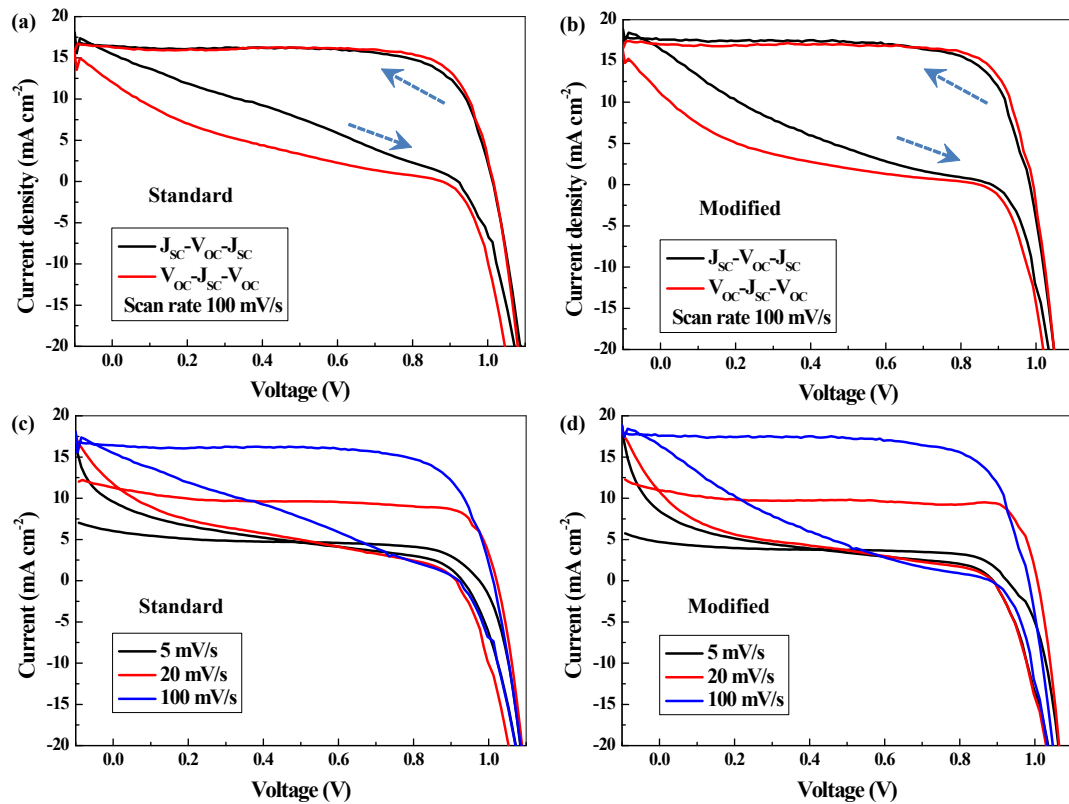


Fig. S3 J-V curves of the PSCs in different cyclic scan directions and scan rates. In the standard PSCs (Fig. S3a), it can be seen that in the scan direction of  $J_{SC}-V_{OC}$ , the photocurrent decreases gradually with the applied voltage increasing, which is similar to the observation in previous reports on trap states induced hysteresis<sup>4,5</sup>. The hysteresis induced by the trap states should be ascribed to the favored recombination current by the trap states which decreases the photocurrent when increasing the applied voltage. As a result, the passivation of the trap states minimizes the carrier loss and leads to the minimized hysteresis. The scan direction of  $V_{OC}-J_{SC}$  leads to normal J-

V behavior which possesses large FF and PCE. In the modified PSCs (Fig. S3b), the scan direction of  $J_{SC}$ - $V_{OC}$  also induces photocurrent decreases with increasing the applied voltage, whereas the shape of the J-V curve is a bit different from the standard PSCs. J-V curve shows a more ‘S’ shape, which is similar to the observations of previous reports on interfacial charge induced hysteresis <sup>6</sup>. By modifying the scan rate, the PSCs present different content of hysteresis. As shown in Fig. S3c and S3d, the hysteresis becomes less obvious with scan rate increasing, just in accordance with the previous observation <sup>7</sup>. The hysteresis in the modified PSCs is probably induced by the interfacial hole accumulation, caused by reduced trap states and enhanced hole extracting of F4TCNQ (Fig. S1d).

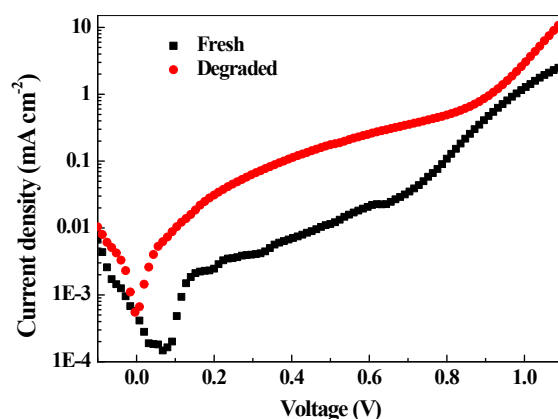


Fig. S4 Dark J-V curves of fresh and degraded standard PSCs. The dark current is increased after degradation, indicating more severe recombination and trap states in the degraded device. Hence, it can be speculated that the bad performance of the degraded device is caused by the increased trap states, implying the probable fact that degradation is assisted by the trap states. Hence, in modified devices, the PSCs with less trap states show improved long-term stability.

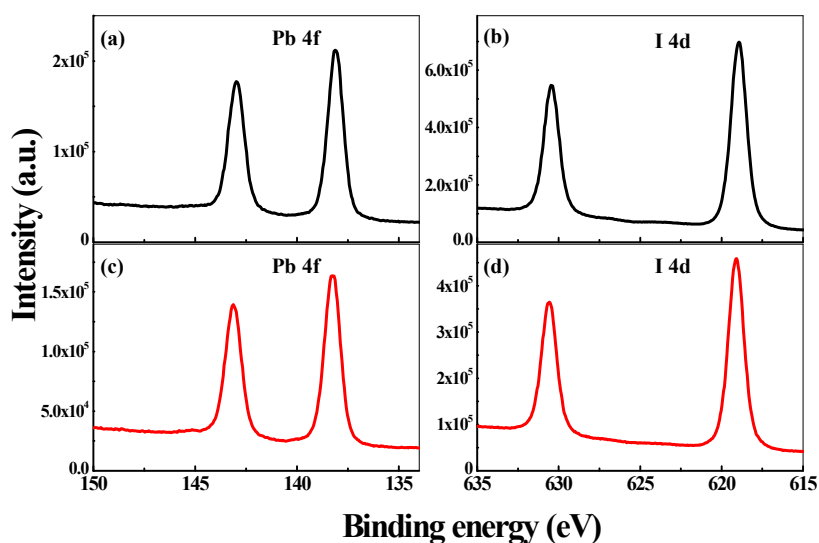


Fig. S5 XPS energy spectra from Pb 4f and I 4d of the standard perovskite film (a, b) and modified perovskite film with F4TCNQ (c, d). The molecular ratio of Pb to I can be calculated by integrating the intensities over the spectra, which is estimated to around 1: 4.

## References

1. Wetzelaer GJA, Scheepers M, Sempere AM, Momblona C, Ávila J, Bolink HJ. Trap-Assisted Non-Radiative Recombination in Organic–Inorganic Perovskite Solar Cells. *Adv. Mater.* 27, 1837-1841 (2015).
2. L. Bertoluzzi, R. S. Sanchez, L. Liu, J. W. Lee, E. Mas-Marza, H. Han, N. G. Park, I. Mora-Sero and J. Bisquert, *Energy Environ. Sci.*, 2015, 8, 910-915.
3. N. G. Park, *Mater. Today*, 2014, 18, 65–72.
4. Shao Y, Xiao Z, Bi C, Yuan Y, Huang J. Origin and elimination of photocurrent hysteresis by fullerene passivation in CH<sub>3</sub>NH<sub>3</sub>PbI<sub>3</sub> planar heterojunction solar cells. *Nat. Commun.* 5, 5784-5784 (2014).
5. Xu J, *et al.* Perovskite-fullerene hybrid materials suppress hysteresis in planar diodes. *Nat. Commun.* 6, 7081 (2015).
6. Zhao Y, *et al.* Anomalously large interface charge in polarity switchable photovoltaic devices: an indication of mobile ions in organic–inorganic halide perovskites. *Energy Environ. Sci.* 8, 1256(2015).
7. Unger E L, *et al.* Hysteresis and transient behavior in current–voltage measurements of hybrid-perovskite absorber solar cells. *Energy Environ. Sci.* 7, 3690 (2014).